Effects of Fullerene Substituents on Structure and Photoelectrochemical Properties of Fullerene Nanoclusters Electrophoretically Deposited on Nanostructured SnO_2 Electrodes

Hiroki Hotta,[†] Soonchul Kang,[‡] Tomokazu Umeyama,[‡] Yoshihiro Matano,[‡] Kaname Yoshida,[§] Seiji Isoda,[§] and Hiroshi Imahori*[,†,‡,||]

PRESTO, Japan Science and Technology Agency, Japan, Department of Molecular Engineering, Graduate School of Engineering, Kyoto University, Katsura, Nishikyo-ku, Kyoto 615-8510, Japan, Institute for Chemical Research, Kyoto University, Uji, Kyoto 611-0011, Japan, and Fukui Institute for Fundamental Chemistry, Kyoto University, 34-4, Takano-Nishihiraki-cho, Sakyo-ku, Kyoto 606-8103, Japan

Received: November 18, 2004; In Final Form: January 24, 2005

Two kinds of fullerene derivatives have been designed to examine the effect of the fullerene substituents on the structure and photoelectrochemical properties of fullerene clusters electrophoretically deposited on nanostructured SnO_2 electrodes. The cluster sizes increase and the incident photon-to-current efficiencies decrease with introduction of large substituents into C_{60}. The trend for photocurrent generation efficiency as well as surface morphology on the electrode can be explained by the steric bulkiness around the C_{60} molecules. A C_{60} molecule with two alkoxy chains is suggested to give a bilayer vesicle structure, irrespective of the hydrophobic nature of both the C_{60} and alkoxy chain moieties. Such information will be valuable for the design of photoactive molecules, which are fabricated onto electrode surfaces to exhibit high energy conversion efficiency.

Introduction

Photochemical and photophysical properties of fullerenes and their derivatives have been extensively studied because of their interesting optical and redox properties.[1,2] Fullerenes have small reorganization energies of electron transfer (ET), which lead to remarkable acceleration of photoinduced charge separation (CS) and of charge shift as well as deceleration of charge recombination.[3,4] Thus, they have been frequently employed as an acceptor in donor−acceptor-linked systems to yield a long-lived charge-separated state with a high quantum yield.[1−5] Significant efforts have also been made in recent years to explore the photovoltaic and photoelectrochemical properties of fullerenes and their derivatives.[6,7] To optimize the performance it is important to (i) harvest the light in the UV−visible regions intensively, (ii) generate a charge-separated state efficiently, and (iii) inject resultant electron and hole into respective electrodes, minimizing undesirable charge recombination. Therefore, the fabrication of these fullerenes onto electrode surfaces is a crucial process for controlling the morphology of fullerene assemblies on a molecular scale. Versatile methods such as spin coating,[6,7] evaporation,[8] Langmuir−Blodgett films,[9] layer-by-layer deposition,[10] self-assembled monolayers (SAM),[11−13] electrophoretic deposition,[14,15] and others[16] have been applied to construct photoelectrochemical devices. In particular, electrophoretic deposition of fullerene clusters in mixed solvents[14] on nanostructured SnO_2 electrodes seems to be highly promising for controlling three-dimensional architecture of the fullerenes on the electrode surfaces, resulting in efficient photoresponse in UV−visible regions and high light energy conversion efficiency.

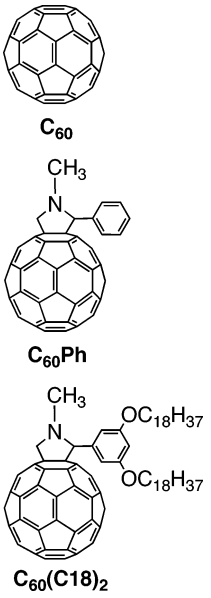

Figure 1. C_{60} and its derivatives used in this study.

Clusters of fullerene,[14a,b] C_{60}−aniline dyad,[14c] and C_{60}−porphyrin composites[15] in toluene/acetonitrile mixed solutions have been deposited electrophoretically onto nanostructured SnO_2 electrodes to exhibit efficient photocurrent generation. Although the film morphology and photoelectrochemical properties of the fullerene-modified SnO_2 electrodes may be influenced by other surrounding fullerenes in the films, the substituent effects of fullerene derivatives in the films have not been fully addressed.

We report herein the effects of fullerene substituents on the structure and photoelectrochemical properties of fullerene clusters electrophoretically deposited on nanostructured SnO_2 electrodes (Figure 1) on the basis of UV−visible absorption, dynamic light scattering (DLS), atomic force microscopy

* Corresponding author: e-mail imahori@scl.kyoto-u.ac.jp.
[†] PRESTO, Japan Science and Technology Agency.
[‡] Department of Molecular Engineering, Graduate School of Engineering, Kyoto University.
[§] Institute for Chemical Research, Kyoto University.
[||] Fukui Institute for Fundamental Chemistry, Kyoto University.

10.1021/jp044725r CCC: $30.25
Published on Web 03/08/2005

(AFM), transmission electron microscopy (TEM), and photoelectrochemical measurements. To evaluate the substituent effects, we designed two fullerene derivatives [$C_{60}(C18)_2$ and C_{60}Ph**]** where a phenylpyrrolidine group with or without long alkoxy groups at the *meta* positions of the phenyl ring is attached on the C_{60} surface by the Prato method.[17] Such substituents would affect the packing structure of the fullerene derivatives in the clusters, exhibiting different film morphologies and photoelectrochemical properties. Thus, comparison of the two fullerene derivatives with pristine C_{60} provides valuable information on the effects of fullerene substituents on the structures and photoelectrochemical properties of fullerene-modified electrodes.

Experimental Section

Materials and Methods. C_{60} (99.5%) was obtained from Term USA. Nanostructured SnO_2 film was prepared by spraying a dilute (1.5%) SnO_2 colloidal solution (particle size 15 nm; Chemat Technology, Inc.) on an optically transparent indium−tin oxide electrode (ITO; Tokyo Sanyo Sinku), which was washed by sonication in 2-propanol and cleaning in an O_3 atmosphere in advance, and finally it was annealed at 673 K (denoted as ITO/SnO_2). Fullerene derivatives C_{60}Ph and $C_{60}(C18)_2$ were prepared by the same procedure as described previously[7b,17] (see S1−S3 in Supporting Information). All other chemicals were of analytical grade and were used as received.

Preparation of Cluster Solutions and Films. The cluster suspensions of fullerenes were prepared in a 1-cm cuvette by injecting 0.5 mL of a toluene solution of fullerenes (0.5 mM) into 1.5 mL of acetonitrile [toluene:acetonitrile = 1/3 (v/v), final concentration of fullerenes = 0.13 mM]. Two electrodes (ITO and ITO/SnO_2) were kept at a distance of 6 mm by use of a Teflon spacer and set in the cuvette, and then dc voltage (200 V) was applied for 2 min between these two electrodes by use of an ATTO AE-8750 power supply.

Characterization. UV−visible spectra of solutions and films were recorded on a Lambda 900 spectrophotometer (Perkin-Elmer). Distribution of cluster size was evaluated by dynamic light scattering (DLS) on a LB-550 particle size analyzer (Horiba, Japan). Transmission electron micrographs (TEM) were measured by applying a drop of the sample to a carbon-coated copper grid. Images were recorded with a JEM-200CX transmission electron microscope (JEOL, Japan). The surface morphology of the films was observed by atomic force microscopy (AFM) measurements with a Digital Nanoscope III (Veeco, USA) in the tapping mode. The thickness of fullerene films on ITO/SnO_2 was determined by a surface roughness/profile measuring instrument (Surfcom 130A, Accretech).

Electrochemical Measurements. All electrochemical measurements were carried out in a standard three-electrode system by use of an ALS 630a electrochemical analyzer. The casting film was immersed into the electrolyte solution containing 0.5 M LiI and 0.01 M I_2 in acetonitrile as a working electrode. Pt wire covered with glass ruggin capillary whose tip was located near the working electrode and Pt coil were used as quasi-reference and counter electrodes, respectively. The potential measured was converted to the saturated calomel electrode (SCE) scale by adding +0.05 V. The stability of the reference electrode potential was confirmed under the experimental conditions. A 500-W xenon lamp (XB-50101AA-A; Ushio, Japan) was used as a light source. The monochromatic light through a monochromator (MC-10N; Ritsu, Japan) was illuminated on the modified area of the working electrode (0.20 cm^2) from the backside. The light intensity was monitored by an optical power meter (ML9002A; Anritsu, Japan) and corrected.

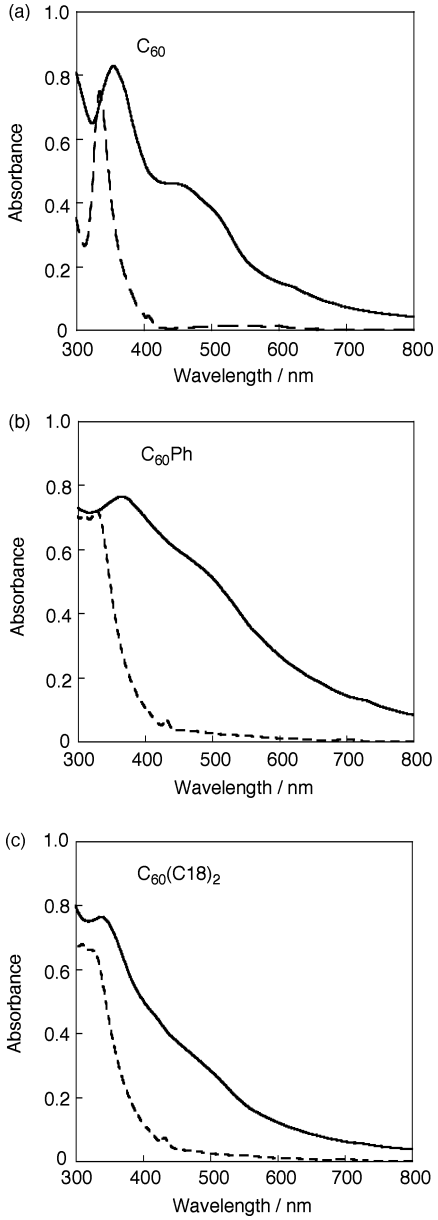

Figure 2. Absorption spectra of (a) C_{60}, (b) C_{60}Ph, and (c) $C_{60}(C18)_2$ in toluene (0.13 mM, − − −) and their cluster solutions [0.13 mM in 1:3 (v/v) toluene/acetonitrile, −]. A 1-mm cell was used for all measurements.

Results and Discussion

Preparation and Characterization of Fullerene Clusters. C_{60} and their derivatives C_{60}Ph and $C_{60}(C18)_2$ form optically transparent clusters in a mixture of toluene/acetonitrile after rapid injection of the toluene solution into acetonitrile [denoted as $(C_{60})_m$, $(C_{60}Ph)_m$, and $[C_{60}(C18)_2]_m$]. Figure 2 displays the absorption spectra of equimolar solutions of C_{60}, C_{60}Ph, and $C_{60}(C18)_2$ in toluene (− − −) and in a toluene/acetonitrile (1:3 v/v) mixture (−). The monoadducts C_{60}Ph and $C_{60}(C18)_2$ in toluene have strong UV bands ($\epsilon_{max} \sim 10^5$ M^{-1} cm^{-1}) as well as a broad and weak visible region similar to C_{60} in toluene. Characteristic absorption bands due to monoadducts[3] appear near 430 and 710 nm for C_{60}Ph and $C_{60}(C18)_2$. Compared to the monomeric form in toluene, clusters of C_{60}, C_{60}Ph, and $C_{60}(C18)_2$ in the toluene/acetonitrile mixture exhibit structureless broad absorption in the 400−800 nm region with higher molar extinction coefficients. These results confirm that these fullerenes aggregate and form clusters in the mixed solvents as reported previously.[14,18,19] Particle size of these clusters in the mixed

TABLE 1: Cluster Size Determined from Various Measurements

	DLS mean diameter/nm	TEM size/nm	AFM[a] horizontal size/nm	AFM[a] vertical size/nm	AFM[b] size/nm
C_{60}	160	100−160	c	c	100−160
$C_{60}Ph$	210	200−320	c	c	160−260
$C_{60}(C18)_2$	270	530−700	470−700	∼20	450−700

[a] Prepared by solvent evaporation of the cluster solutions on mica. [b] Prepared by electrophoretic deposition of the cluster solutions onto ITO/SnO_2. [c] Not measured.

solvent was measured by dynamic light scattering (DLS). In a mixture (1:3) of toluene/acetonitrile at an incubation time of 10 min after the rapid injection, the size distribution of $(C_{60})_m$, $(C_{60}Ph)_m$, and $[C_{60}(C18)_2]_m$ clusters was found to be relatively narrow with different mean diameters (D_M) of 160 nm for $(C_{60})_m$, 210 nm for $(C_{60}Ph)_m$, and 270 nm for $[C_{60}(C18)_2]_m$ (Figure 3A and Table 1). The order of the mean diameters [i.e., C_{60} < $C_{60}Ph$ < $C_{60}(C18)_2$] is consistent with that of their molecular sizes. The mean diameters of $(C_{60})_m$ and $(C_{60}Ph)_m$ also agree with the previously reported values of $(C_{60})_m$ (150 nm)[14a] and clusters of similar fullerene derivatives (160−180 nm).[14c] It is noteworthy that the mean diameter of $[C_{60}(C18)_2]_m$ is significantly larger than those of clusters of $(C_{60})_m$ and $(C_{60}Ph)_m$. In addition, the size distribution of clusters of $[C_{60}(C18)_2]_m$ increases with increasing incubation time (Figure 3B), whereas those of $(C_{60})_m$ and $(C_{60}Ph)_m$ virtually remain the same. These results suggest that $C_{60}(C18)_2$ molecules are associated with the help of two long alkoxy chains to make aggregates in the mixed solvent.

To assess the shape and morphology of the $(C_{60})_m$, $(C_{60}Ph)_m$, and $[C_{60}(C18)_2]_m$ clusters, we performed transmission electron microscopy (TEM) and atomic force microscopy (AFM) measurements. Figure 4 shows the TEM images of the clusters prepared by the deposition of $(C_{60})_m$, $(C_{60}Ph)_m$, and $[C_{60}(C18)_2]_m$ in toluene/acetonitrile mixed solvents on a carbon-coated copper grid. The clusters of $(C_{60})_m$ and $(C_{60}Ph)_m$ form network structures with small particles. The sizes of small particles for $(C_{60})_m$ (100−160 nm) and $(C_{60}Ph)_m$ (200−320 nm) are similar to the corresponding values determined from DLS measurements (Table 1). On the other hand, the clusters of $[C_{60}(C18)_2]_m$ are spherical with large size (530−700 nm) relative to the mean diameter determined from DLS measurements (Table 1). These results also indicate that as solvent evaporates on the grid, secondary aggregation occurs in an orderly fashion to form large aggregates with the help of two long alkoxy chains. Recent studies of amphiphilic fullerene derivatives reported hollow spherical morphology that mimics the geometry of bilayer vesicles.[20] Taking into account the fact that the TEM image of $[C_{60}(C18)_2]_m$ is much thinner than those of $(C_{60})_m$ and $(C_{60}Ph)_m$, we propose that $C_{60}(C18)_2$ molecules in the mixed solvents form vesicles made of bilayers with head([60]fullerene)-to-tail (two alkoxy groups) conformation.

To get more information on the structure of $[C_{60}(C18)_2]_m$ clusters, AFM measurement was also carried out for the sample prepared by evaporation of $[C_{60}(C18)_2]_m$ cluster solutions on mica surface. The AFM image of the $[C_{60}(C18)_2]_m$ cluster reveals a disklike structure with thickness of ∼20 nm (Figure

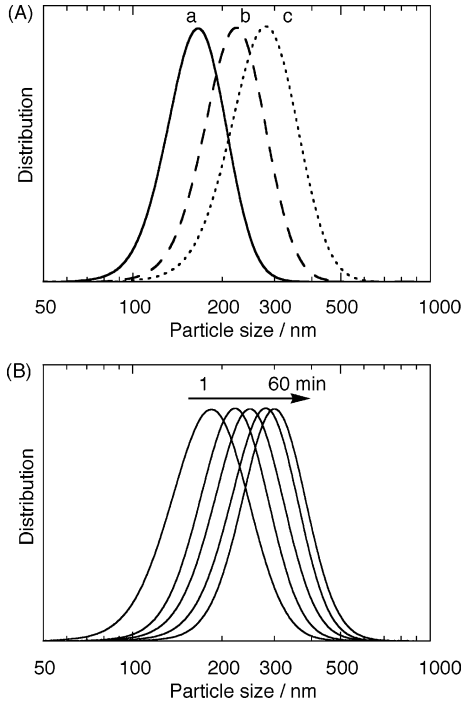

Figure 3. (A) Particle size distribution of clusters (0.13 mM) of (a) C_{60} (—), (b) $C_{60}Ph$ (− − −), and (c) $C_{60}(C18)_2$ (···) in 1:3 (v/v) toluene/acetonitrile mixture at 10 min after rapid injection of the toluene solutions into acetonitrile. (B) Particle size distribution of clusters (0.13 mM) of $C_{60}(C18)_2$ in 1:3 (v/v) toluene/acetonitrile mixture at 1, 3, 5, 10, and 60 min after rapid injection of $C_{60}(C18)_2$ toluene solution into acetonitrile.

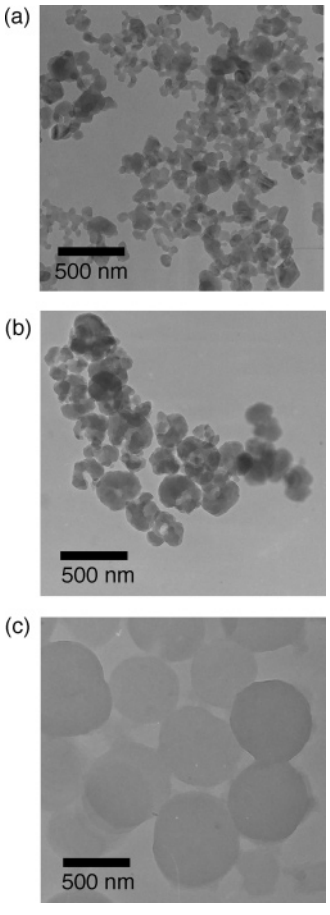

Figure 4. TEM images of (a) $(C_{60})_m$, (b) $(C_{60}Ph)_m$, and (c) $[C_{60}(C18)_2]_m$.

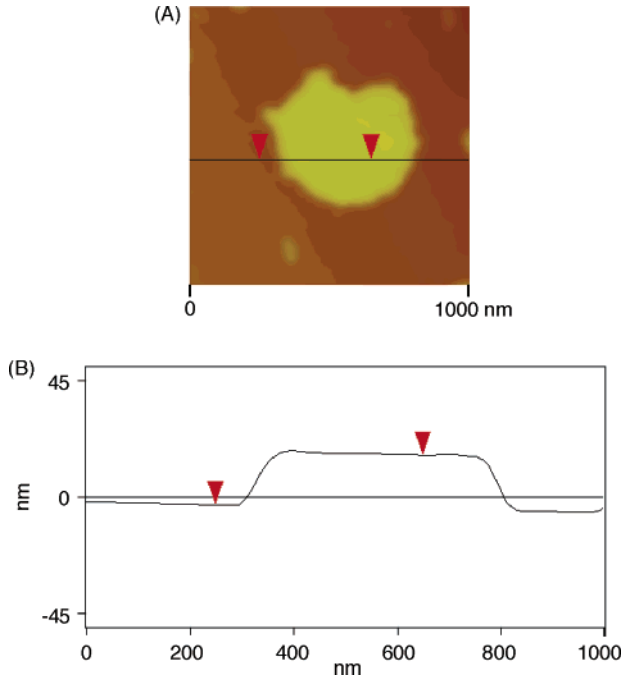

Figure 5. (A) AFM image of $[C_{60}(C18)_2]_m$ on mica and (B) a section profile of the AFM image.

5). The horizontal size of the $[C_{60}(C18)_2]_m$ cluster (470−700 nm) agrees with that determined from TEM measurements (Table 1). It should be emphasized here that the vertical size of $[C_{60}(C18)_2]_m$ (∼20 nm) is much smaller than horizontal value of $[C_{60}(C18)_2]_m$. The molecular length of $C_{60}(C18)_2$, estimated from CPK space-filling model, is ∼4 nm. Although detailed structure at the molecular level is not yet clear, self-organization of $C_{60}(C18)_2$ in the mixed solvent would result in the formation of bilayer vesicle with a thickness of ∼8 nm, which is 2 times larger than the molecular length of $C_{60}(C18)_2$. In such a case solvent evaporation from the inner space of the bilayer vesicle may yield the disklike structure with thickness of ∼20 nm, which largely agrees with thickness of double bilayer made from $C_{60}(C18)_2$. It is interesting to note that the C_{60} and alkoxy chain moieties are both hydrophobic to give bilayer vesicles, which are typically made from amphiphilic fullerene derivatives.[20,21] C_{60} bearing artificial lipids with three long alkyl chains is reported to form bilayer structures with head([60]fullerene)-to-tail (two alkoxy groups) conformation in the cast films.[21c]

Electrophoretic Deposition of Fullerene Clusters. Clusters of C_{60} and fullerene derivatives can be deposited electrophoretically onto nanostructured SnO_2 electrode by applying dc voltage to the electrode.[14,15] In a similar manner, the clusters of C_{60}, C_{60}Ph, and $C_{60}(C18)_2$ are attached onto ITO/SnO_2 electrodes by the electrophoretic deposition method [denoted as ITO/SnO_2/$(C_{60})_n$, ITO/SnO_2/$(C_{60}Ph)_n$, and ITO/SnO_2/$[C_{60}(C18)_2]_n$, respectively]. Under application of a high dc electric field (200 V for 2 min), clusters of C_{60} and the fullerene derivatives in toluene/acetonitrile become negatively charged as they are driven toward the positively charged electrode surface.[22] With increasing time of deposition, the ITO/SnO_2 electrode turns brown in color, whereas discoloration of the cluster solution takes place. As a result, cluster films with a thickness of 2∼3 μm could be obtained. Absorption spectra of cluster films on nanostructured SnO_2 electrode are shown in Figure 6. The absorption features of ITO/SnO_2/$(C_{60})_n$, ITO/SnO_2/$(C_{60}Ph)_n$, and ITO/SnO_2/$[C_{60}(C18)_2]_n$ are similar to those observed for cluster solutions in the toluene/acetonitrile mixture (solid lines in Figure 2). The broad absorption of these films as well as high molar absorptivity in the visible and near-IR regions makes these films suitable for harvesting solar energy.

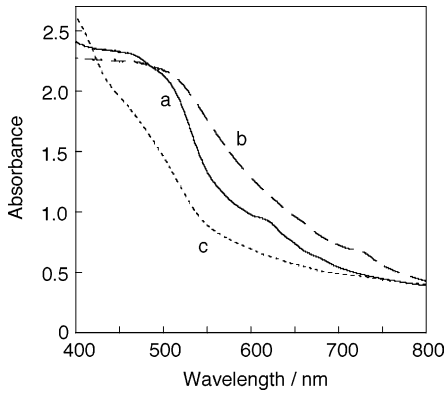

Figure 6. Absorption spectra of (a) ITO/SnO_2/$(C_{60})_n$ (—), (b) ITO/SnO_2/$(C_{60}Ph)_n$ (− − −), and (c) ITO/SnO_2/$[C_{60}(C18)_2]_n$ (···).

AFM was used to evaluate the topology of ITO/SnO_2/$(C_{60})_n$, ITO/SnO_2/$(C_{60}Ph)_n$, and ITO/SnO_2/$[C_{60}(C18)_2]_n$ films as shown in Figure 7. The ITO/SnO_2/$(C_{60})_n$, ITO/SnO_2/$(C_{60}Ph)_n$, and ITO/SnO_2/$[C_{60}(C18)_2]_n$ films are composed of closely packed clusters with sizes of 100−160, 160−260, and 450−700 nm, respectively. The order of the cluster sizes matches that of the molecular sizes, and the cluster sizes are nearly the same as those measured by TEM (Table 1). It should be noted here that the AFM image of ITO/SnO_2/$[C_{60}(C18)_2]_n$ films reveals a disklike structure, which is in good agreement with the AFM image of $[C_{60}(C18)_2]_n$ on mica (vide supra).

Photoelectrochemical Measurements. Photoelectrochemical measurements were performed in acetonitrile containing 0.5 M LiI and 0.01 M I_2 with ITO/SnO_2/$(C_{60})_n$, ITO/SnO_2/$(C_{60}Ph)_n$, or ITO/SnO_2/$[C_{60}(C18)_2]_n$, as a working electrode, a platinum counter electrode, and a reference electrode. Figure 8 displays anodic photocurrent responses of the fullerene films illuminated at an excitation wavelength of 450 nm (input power 25 μW cm^{-2}) at 0.11 V vs SCE. The photocurrent responses are prompt, steady, and reproducible during repeated on/off cycles of visible light illumination. Blank experiments conducted with ITO/SnO_2 produced no detectable photocurrent under similar experimental conditions. These results demonstrate the role of fullerene assemblies toward harvesting light energy and generating photocurrent during the operation of a photoelectrochemical device. The intensities of photocurrent under the same conditions are in the order ITO/SnO_2/$(C_{60})_n$ > ITO/SnO_2/$(C_{60}Ph)_n$ > ITO/SnO_2/$[C_{60}(C18)_2]_n$ devices (vide infra). Current versus potential characteristics of ITO/SnO_2/$(C_{60})_n$, ITO/SnO_2/$(C_{60}Ph)_n$, and ITO/SnO_2/$[C_{60}(C18)_2]_n$ devices were also examined under the same illumination conditions (see Figure S1 in Supporting Information). With increasing positive bias, the photocurrent increases as compared to the dark current. Increased charge separation and the facile transport of charge carriers under positive bias are responsible for enhanced photocurrent generation.

To evaluate the response of fullerene clusters toward photocurrent generation, a series of photocurrent action spectra were recorded and compared against the absorption spectra. The photocurrent action spectra of ITO/SnO_2/$(C_{60})_n$, ITO/SnO_2/$(C_{60}Ph)_n$, and ITO/SnO_2/$[C_{60}(C18)_2]_n$ devices are shown in Figure 9. IPCE values were calculated by normalizing the photocurrent densities for incident light energy and intensity and by use of the expression

$$\text{IPCE (\%)} = 100 \times 1240 \times i/(W_{in} \times \lambda)$$

where i is the photocurrent density (A cm^{-2}), W_{in} is the incident

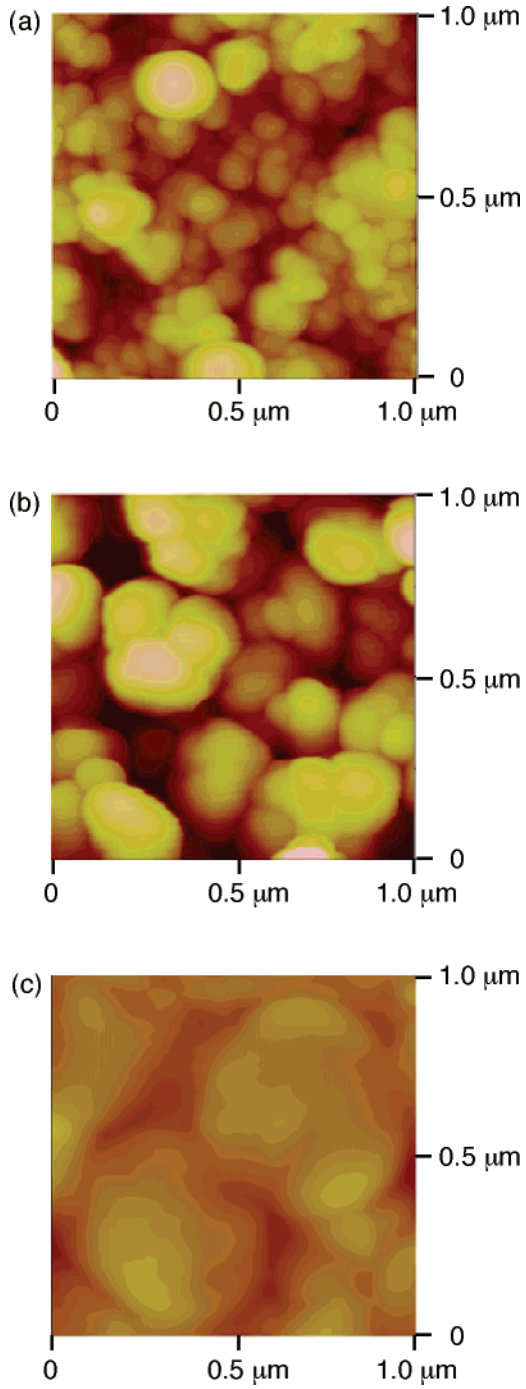

Figure 7. AFM images of (a) ITO/SnO_2/$(C_{60})_n$, (b) ITO/SnO_2/$(C_{60}Ph)_n$, and (c) ITO/SnO_2/$[C_{60}(C18)_2]_n$ electrodes.

light intensity (W cm^{-2}), and λ is the excitation wavelength (nm). The overall responses of ITO/SnO_2/$(C_{60})_n$, ITO/SnO_2/$(C_{60}Ph)_n$, and ITO/SnO_2/$[C_{60}(C18)_2]_n$ devices parallel the broad absorption features, indicating the involvement of the C_{60} moiety in photocurrent generation. These results agree well with photoelectrochemical properties of similar C_{60} devices.[14] It is intriguing to compare the IPCE values between the three different photoelectrochemical devices. The maximum IPCE values at an excitation wavelength of 400 nm decrease in the order ITO/SnO_2/$(C_{60})_n$ (2.3%) > ITO/SnO_2/$(C_{60}Ph)_n$ (1.1%) > ITO/SnO_2/$[C_{60}(C18)_2]_n$ (0.3%). These results reveal that photocurrent generation efficiency decreases with introduction of large substituents onto C_{60} surface.

Photocurrent Generation Mechanism. Based on previous studies of a similar photoelectrochemical system of C_{60} and

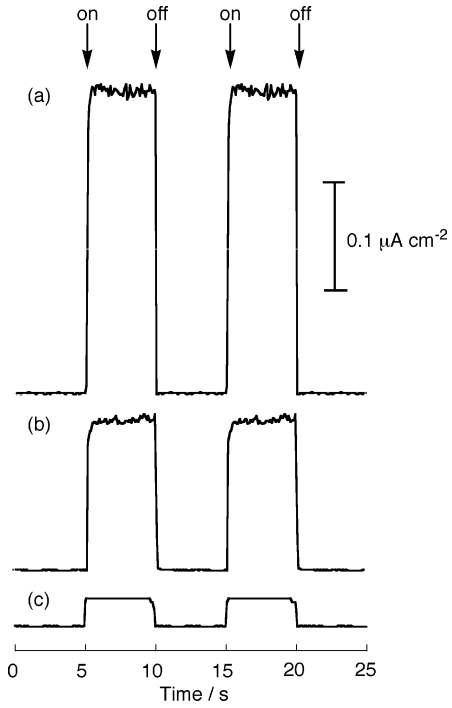

Figure 8. Photocurrent response of (a) ITO/SnO_2/$(C_{60})_n$, (b) ITO/SnO_2/$(C_{60}Ph)_n$, and (c) ITO/SnO_2/$[C_{60}(C18)_2]_n$ electrodes at λ_{ex} = 450 nm. Potential, +0.11 V vs SCE; 0.5 M LiI and 0.01 M I_2 in acetonitrile; input power, 25 μW cm^{-2}.

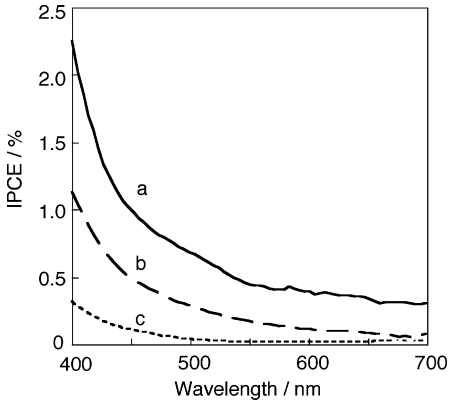

Figure 9. Action spectra of (a) ITO/SnO_2/$(C_{60})_n$ (—), (b) ITO/SnO_2/$(C_{60}Ph)_n$ (– – –), and (c) ITO/SnO_2/$[C_{60}(C18)_2]_n$ (•••) electrodes. Potential, +0.11 V vs SCE; 0.5 M LiI and 0.01 M I_2 in acetonitrile.

fullerene derivatives,[14] a photocurrent generation diagram is schematically illustrated in Figure 10. First reduction potentials of $C_{60}Ph$ and $C_{60}(C18)_2$ (−0.3 V vs NHE) were determined by cyclic voltammetry in CH_2Cl_2 containing 0.1 M tetrabutylammonium hexafluorophosphate. Photoinduced electron transfer between iodide ion (I_3^-/I^- = 0.5 V vs NHE)[14] and the excited states of C_{60} clusters ($^1C_{60}^*$ = 1.5∼1.7 V vs NHE; $^3C_{60}^*$ = 1.2∼1.4 V vs NHE)[14] is the primary step in the photocurrent generation.[14a,23] The reduced C_{60} ($C_{60}/C_{60}^{\bullet-}$ = −0.2 ∼ −0.3 V vs NHE)[14] then injects electrons into SnO_2 nanocrystallites (E_{CB} = 0 V vs NHE).[14] The electrons transferred to the semiconductor nanocrystallines are driven to the counter electrode via external circuit to regenerate the redox couple. The maximum IPCE values at excitation wavelength of 400 nm decrease in the order ITO/SnO_2/$(C_{60})_n$ (2.3%) > ITO/SnO_2/$(C_{60}Ph)_n$ (1.1%) > ITO/SnO_2/$[C_{60}(C18)_2]_n$ (0.3%). The first reduction potentials of $C_{60}Ph$ and $C_{60}(C18)_2$ are more negative by ∼0.1 V than that of C_{60} itself (−0.2 V vs NHE).[14a] In the primary step, driving forces for photoinduced electron transfer from I^- to the excited states

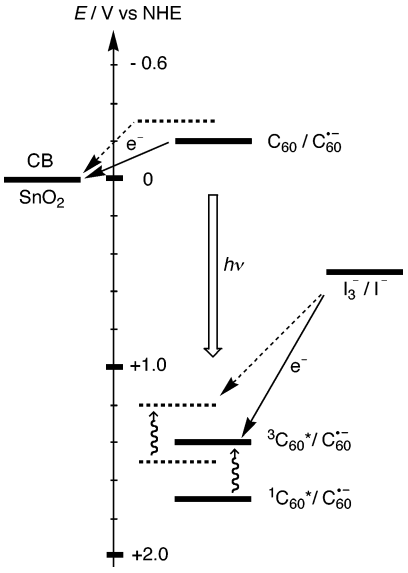

Figure 10. Photocurrent generation diagram for the fullerene photoelectrochemical devices. Solid and broken bars correspond to ITO/SnO_2/$(C_{60})_n$ and ITO/SnO_2/$(C_{60}Ph)_n$ or $[C_{60}(C18)_2]_n$ devices, respectively.

of the C_{60} clusters are more exothermic in ITO/SnO_2/$(C_{60}Ph)_n$ and ITO/SnO_2/$[C_{60}(C18)_2]_n$ devices by 0.2 V than the values in the ITO/SnO_2/$(C_{60})_n$ device. However, the driving forces are relatively large (>0.7 V) so that the ET processes are likely to be located in the Marcus top region, where the ET rates are governed by the diffusion-limited process. Accordingly, the difference in the driving forces would not affect the electron transfer rates significantly among the three systems. On the other hand, in the secondary electron-transfer step, the driving forces from $C_{60}^{\bullet-}$ to the conduction band of the SnO_2 nanocrystallites are relatively small (0.2∼0.3 V) so that the electron-transfer rates in ITO/SnO_2/$(C_{60}Ph)_n$ and ITO/SnO_2/$[C_{60}(C18)_2]_n$ devices would be much larger than the value in ITO/SnO_2/$(C_{60})_n$ device, because they are positioned in the Marcus normal region. In such a case, IPCE values of ITO/SnO_2/$(C_{60}Ph)_n$ and ITO/SnO_2/$[C_{60}(C18)_2]_n$ devices may be enhanced relative to the ITO/SnO_2/$(C_{60})_n$ device. Since the IPCE values of ITO/SnO_2/$(C_{60}Ph)_n$ and ITO/SnO_2/$[C_{60}(C18)_2]_n$ devices are much smaller than that of the ITO/SnO_2/$(C_{60})_n$ device, the steric factor on the C_{60} moiety may be responsible for the trend in photocurrent generation efficiency. In other words, with introduction of larger substituents on the C_{60} moiety, the separation distance between the ET couples increases. Thus, the ET rates between the C_{60} molecules and the electrode or I^- as well as the C_{60} molecules are slowed, lowering the IPCE values.

In conclusion, we have successfully elucidated the relationship between molecular structures, surface morphology of their molecular aggregates on the nanostructured semiconductor electrode, and their photoelectrochemical properties. The trend for the photocurrent generation efficiency as well as the surface morphology on the electrode can be rationalized by the steric bulkiness around the C_{60} molecules. C_{60} molecule with two alkoxy chains in toluene/acetonitrile is suggested to give a bilayer vesicle structure, irrespective of the hydrophobic nature of both C_{60} and alkoxy chain moieties. Such information will be valuable for the design of photoactive molecules that are fabricated onto electrode surfaces to exhibit unique photophysical and photoelectrochemical properties.

Acknowledgment. We thank Mr. Naoki Aratani (Kyoto University) for measurements of FAB-MS. This work was supported by a Grant-in-Aid (11740352 to H.I.) from the Ministry of Education, Culture, Sports, Science and Technology (MEXT), Japan. H.I. also thanks Grant-in-Aid from MEXT, Japan (21st Century COE on Kyoto University Alliance for Chemistry) for financial support. A part of this work was supported by "Nanotechnology Support Project" of the Ministry of Education, Culture, Sports, Science and Technology (MEXT), Japan.

Supporting Information Available: Synthetic data and current versus potential curves for photoelectrochemical devices (PDF). This information is available free of charge via the Internet at http://pubs.acs.org.

References and Notes

(1) (a) Martín, N.; Sánchez, L.; Illescas, B.; Pérez, I. *Chem. Rev.* **1998**, *98*, 2527. (b) Prato, M. *J. Mater. Chem.* **1997**, *7*, 1097. (c) Diederich, F.; Gómez-López, M. *Chem. Soc. Rev.* **1999**, *28*, 263. (d) Sun, Y.-P.; Riggs, J. E.; Guo, Z.; Rollins, H. W. In *Optical and Electronic Properties of Fullerenes and Fullerene-Based Materials*; Shinar, J., Vardeny, Z. V., Kafafi, Z. H., Eds.; Marcel Dekker: New York, 2000; pp 43−81.

(2) (a) Guldi, D. M.; Kamat, P. V. In *Fullerenes*; Kadish, K. M., Ruoff, R. S., Eds.; John Wiley & Sons: New York, 2000; Chapt. 5, pp 225−281. (b) Fukuzumi, S.; Guldi, D. M. In *Electron Transfer in Chemistry*; Balzani, V. Ed.; Wiley−VCH: Weinheim, Germany, 2001; Vol. 2, pp 270−337. (c) Gust, D.; Moore, T. A.; Moore, A. L. *Acc. Chem. Res.* **2001**, *34*, 40. (d) Nierengarten, N.-F. *New J. Chem.* **2004**, *28*, 1177. (e) Armaroli, N. *Photochem. Photobiol. Sci.* **2003**, *2*, 73.

(3) (a) Imahori, H.; Sakata, Y. *Adv. Mater.* **1997**, *9*, 537. (b) Imahori, H.; Sakata, Y. *Eur. J. Org. Chem.* **1999**, 2445. (c) Imahori, H. *Org. Biomol. Chem.* **2004**, *2*, 1425. (d) Imahori, H. *J. Phys. Chem. B* **2004**, *108*, 6130. (e) Imahori, H.; Fukuzumi, S. *Adv. Funct. Mater.* **2004**, *14*, 525.

(4) (a) Imahori, H.; Hagiwara, K.; Akiyama, T.; Aoki, M.; Taniguchi, S.; Okada, T.; Shirakawa, M.; Sakata, Y. *Chem. Phys. Lett.* **1996**, *263*, 545. (b) Imahori, H.; Tamaki, K.; Guldi, D. M.; Luo, C.; Fujitsuka, M.; Ito, O.; Sakata, Y.; Fukuzumi, S. *J. Am. Chem. Soc.* **2001**, *123*, 2607. (c) Imahori, H.; Guldi, D. M.; Tamaki, K.; Yoshida, Y.; Luo, C.; Sakata, Y.; Fukuzumi, S. *J. Am. Chem. Soc.* **2001**, *123*, 6617. (d) Imahori, H.; Tkachenko, N. V.; Vehmanen, V.; Tamaki, K.; Lemmetyinen, H.; Sakata, Y.; Fukuzumi, S. *J. Phys. Chem. A* **2001**, *105*, 1750. (e) Imahori, H.; Yamada, H.; Guldi, D. M.; Endo, Y.; Shimomura, A.; Kundu, S.; Yamada, K.; Okada, T.; Sakata, Y.; Fukuzumi, S. *Angew. Chem., Int. Ed.* **2002**, *41*, 2344.

(5) (a) Choi, M.-S.; Aida, T.; Luo, H.; Araki, Y.; Ito, O. *Angew. Chem., Int. Ed.* **2003**, *42*, 4060. (b) Li, K.; Schuster, D. I.; Guldi, D. M.; Herranz, M. A.; Echegoyen, L. *J. Am. Chem. Soc.* **2004**, *126*, 3388. (c) D'Souza, F.; Deviprasad, G. R.; El-Khouly, M. E.; Fujitsuka, M.; Ito, O. *J. Am. Chem. Soc.* **2001**, *123*, 5277. (d) Armaroli, N.; Marconi, G.; Echegoyen, L.; Bourgeois, J.-P.; Diederich, F. *Chem. Eur. J.* **2000**, *6*, 1629. (e) D'Souza, F.; Smith, P. M.; Zandler, M. E.; McCarty, A. L.; Itou, M.; Araki, Y.; Ito, O. *J. Am. Chem. Soc.* **2004**, *126*, 7898.

(6) (a) Yu, G.; Gao, J.; Hummelen, J. C.; Wudl, F.; Heeger, A. J. *Science* **1995**, *270*, 1789. (b) Shaheen, S. E.; Brabec, C. J.; Sariciftci, N. S.; Padinger, F.; Fromherz, T.; Hummelen, J. C. *Appl. Phys. Lett.* **2001**, *78*, 841. (c) Padinger, F.; Rittberger, R. S.; Sariciftci, N. S. *Adv. Funct. Mater.* **2003**, *13*, 85.

(7) (a) Wienk, M. M.; Kroon, J. M.; Verhees, W. J. H.; Knol, J.; Hummelen, J. C.; van Hal, P. A.; Janssen, R. A. J. *Angew. Chem., Int. Ed.* **2003**, *42*, 3371. (b) Eckert, J.-F.; Nicoud, J.-F.; Nierengarten, J.-F.; Liu, S.-G.; Echegoyen, L.; Barigelletti, F.; Armaroli, N.; Ouali, L.; Krasnikov, V.; Hadziioannou, G. *J. Am. Chem. Soc.* **2000**, *122*, 7467.

(8) Tsuzuki, T.; Shirota, Y.; Rostalski, J.; Meissner, D. *Solar Energy Mater. Solar Cells* **2000**, *61*, 1.

(9) (a) Luo, C.; Huang, C.; Gan, L.; Zhou, D.; Xia, W.; Zhuang, Q.; Zhao, Y.; Huang, Y. *J. Phys. Chem. B* **1996**, *100*, 16685. (b) Zhang, W.; Shi, Y.; Gan, L.; Huang, C.; Luo, H.; Wu, D.; Li, N. *J. Phys. Chem. B* **1999**, *103*, 675.

(10) Luo, C.; Guldi, D. M.; Maggini, M.; Menna, E.; Mondini, S.; Kotov, N. A.; Prato, M. *Angew. Chem., Int. Ed.* **2000**, *39*, 3905.

(11) (a) Imahori, H.; Azuma, T.; Ajavakom, A.; Norieda, H.; Yamada, H.; Sakata, Y. *J. Phys. Chem. B* **1999**, *103*, 7233. (b) Imahori, H.; Yamada, H.; Nishimura, Y.; Yamazaki, I.; Sakata, Y. *J. Phys. Chem. B* **2000**, *104*, 2099. (c) Imahori, H.; Norieda, H.; Yamada, H.; Nishimura, Y.; Yamazaki, I.; Sakata, Y.; Fukuzumi, S. *J. Am. Chem. Soc.* **2001**, *123*, 100. (d) Hirayama, D.; Takimiya, K.; Aso, Y.; Otsubo, T.; Hasobe, T.; Yamada, H.; Imahori, H.; Fukuzumi, S.; Sakata, Y. *J. Am. Chem. Soc.* **2002**, *124*, 532.

(12) (a) Yamada, H.; Imahori, H.; Nishimura, Y.; Yamazaki, I.; Fukuzumi, S. *Adv. Mater.* **2002**, *14*, 892. (b) Yamada, H.; Imahori, H.;

Nishimura, Y.; Yamazaki, I.; Ahn, T. K.; Kim, S. K.; Kim, D.; Fukuzumi, S. *J. Am. Chem. Soc.* **2003**, *125*, 9129. (c) Imahori, H.; Kimura, M.; Hosomizu, K.; Sato, T.; Ahn, T. K.; Kim, S. K.; Kim, D.; Nishimura, Y.; Yamazaki, I.; Araki, Y.; Ito, O.; Fukuzumi, S. *Chem. Eur. J.* **2004**, *10*, 5111.

(13) (a) Hatano, T.; Ikeda, A.; Akiyama, T.; Yamada, S.; Sano, M.; Kanekiyo, Y.; Shinkai, S. *J. Chem. Soc., Perkin Trans. 2* **2000**, *5*, 909. (b) Ikeda, A.; Hatano, T.; Shinkai, S.; Akiyama, T.; Yamada, S. *J. Am. Chem. Soc.* **2001**, *123*, 4855. (c) Enger, O.; Nuesch, F.; Fibbioli, M.; Echegoyen, L.; Pretsch, E.; Diederich, F. *J. Mater. Chem.* **2000**, *10*, 2231.

(14) (a) Kamat, P. V.; Barazzouk, S.; Thomas, K. G.; Hotchandani, S. *J. Phys. Chem. B* **2000**, *104*, 4014. (b) Kamat. P. V.; Haria, M.; Hotchandani, S. *J. Phys. Chem. B* **2004**, *108*, 5166. (c) Kamat, P. V.; Barazzouk, S.; Hotchandani, S.; Thomas, K. G. *Chem. Eur. J.* **2000**, *6*, 3914.

(15) (a) Imahori, H.; Hasobe, T.; Yamada, H.; Kamat, P. V.; Barazzouk, S.; Fujitsuka, M.; Ito, O.; Fukuzumi, S. *Chem. Lett.* **2001**, 784. (b) Hasobe, T.; Imahori, H.; Fukuzumi, S.; Kamat, P. V. *J. Phys. Chem. B* **2003**, *107*, 12105. (c) Hasobe, T.; Imahori, H.; Kamat, P. V.; Fukuzumi, S. *J. Am. Chem. Soc.* **2003**, *125*, 14962. (d) Hasobe, T.; Kashiwagi, Y.; Absalom, M.; Hosomizu, K.; Crossley, M. J.; Imahori, H.; Kamat, P. V.; Fukuzumi, S. *Adv. Mater.* **2004**, *16*, 975. (e) Hasobe, T.; Kamat, P. V.; Absalom, M. A.; Kashiwagi, Y.; Sly, J.; Crossley, M. J.; Hosomizu, K.; Imahori, H.; Fukuzumi, S. *J. Phys. Chem. B* **2004**, *118*, 12865.

(16) (a) Liu, Y.; Xiao, S.; Li, H.; Li, Y.; Liu, H.; Lu, F.; Zhung, J.; Zhu, D. *J. Phys. Chem. B* **2004**, *108*, 6256. (b) Sudeep, P. K.; Ipe, B. I.; Thomas, K. G.; Geroge, M. V.; Barazzouk, S.; Hotchandani, S.; Kamat, P. V. *Nano Lett.* **2002**, *2*, 29. (c) Imahori, H.; Liu, J.-C.; Hosomizu, K.; Sato, T.; Mori, Y.; Hotta, H.; Matano, Y.; Araki, Y.; Ito, O.; Maruyama, N.; Fujita, S. *Chem. Commun.* **2004**, 2066.

(17) Maggini, M.; Scorrano, G.; Prato, M. *J. Am. Chem. Soc.* **1993**, *115*, 9798.

(18) (a) Wang, Y.-M.; Kamat, P. V.; Patterson, L. K. *J. Phys. Chem.* **1993**, *97*, 8793. (b) Sun, Y.-P.; Ma, B.; Bunker, C. E.; Liu, B. *J. Am. Chem. Soc.* **1995**, *117*, 12705. (c) Nath, S.; Pal, H.; Palit, D. K.; Sapre, A. V.; Mittal, J. P. *J. Phys. Chem. B* **1998**, *102*, 10158.

(19) (a) Thomas, K. G.; Biju, V.; Guldi, D. M.; Kamat, P. V.; George, M. V. *J. Phys. Chem. B* **1999**, *103*, 8864. (b) Biju, V.; Sudeep, P. K.; Thomas, K. G.; George, M. V. *Langmuir* **2002**, *18*, 1831.

(20) (a) Zhou, A.; Burger, C.; Chu, B.; Sawamura, M.; Nagahama, N.; Toganoh, M.; Hackler, U. E.; Isobe, H.; Nakamura, E. *Science* **2001**, *291*, 1944. (b) Sano, M.; Oishi, K.; Ishi-I, T.; Shinkai, S. *Langmuir* **2000**, *16*, 3773. (c) Cassell, A. M.; Asplund, C. L.; Tour, J. M. *Angew. Chem., Int. Ed.* **1999**, *38*, 2403.

(21) (a) Brettreich, M.; Burghardt, S.; Böttcher, C.; Bayerl, T.; Bayerl, S.; Hirsch, A. *Angew. Chem., Int. Ed.* **2000**, *39*, 1845. (b) Nakashima, N.; Ishii, T.; Shirakusa, M.; Nakanishi, T.; Murakami, H.; Sagara, T. *Chem. Eur. J.* **2001**, *7*, 1766. (c) Nakanishi, T.; Morita, M.; Murakami, H.; Sagara, T.; Nakashima, N. *Chem. Eur. J.* **2002**, *8*, 1641. (d) Nakanishi, T.; Ohwaki, H.; Tanaka, H.; Murakami, H.; Sagara, T.; Nakashima, N. *J. Phys. Chem. B* **2004**, *108*, 7754.

(22) Echegoyen et al. have reported an efficient retro-Bingel reaction under mild electrochemical conditions; see, Echegoyen, L. E.; Djojo, F. D.; Hirsch, A.; Echegoyen, L. *J. Org. Chem.* **2000**, *65*, 4994. To confirm the possibility of retro-Prato reaction under high voltage, an absorption spectrum of the deposited ITO/SnO_2/$C_{60}(C18)_2$ redissolved in toluene was measured. The absorption spectrum was the same as that of $C_{60}(C18)_2$ in toluene, demonstrating that the fullerene derivatives electrophoretically deposited on the ITO/SnO_2 are not decomposed by application of high voltage.

(23) Taking into account the fact that the intersystem crossing rate of C_{60} excited singlet state into C_{60} excited triplet state [$(5-7) \times 10^8$ s^{-1}] and the diffusion-limited electron-transfer rate from I^- to the C_{60} excited states [$(2 \times 10^9$ M^{-1} $s^{-1}) \times 10^{-2}$ $M = 2 \times 10^7$ s^{-1}], photocurrent generation in the present system may result from the C_{60} excited triplet state rather than the C_{60} excited singlet state.